Microscopic Theory for the Role of Attractive Forces in the Dynamics of Supercooled Liquids

Zachary E. Dell[1] and Kenneth S. Schweizer[2,3,4,*]
[1]Department of Physics, University of Illinois, Urbana, Illinois 61801, USA
[2]Department of Materials Science, University of Illinois, Urbana, Illinois 61801, USA
[3]Department of Chemistry, University of Illinois, Urbana, Illinois 61801, USA
[4]Frederick Seitz Materials Research Laboratory, University of Illinois, Urbana, Illinois 61801, USA
(Received 16 April 2015; published 11 November 2015)

We formulate a microscopic, no adjustable parameter, theory of activated relaxation in supercooled liquids directly in terms of the repulsive and attractive forces within the framework of pair correlations. Under isochoric conditions, attractive forces can nonperturbatively modify slow dynamics, but at high enough density their influence vanishes. Under isobaric conditions, attractive forces play a minor role. High temperature apparent Arrhenius behavior and density-temperature scaling are predicted. Our results are consistent with recent isochoric simulations and isobaric experiments on a deeply supercooled molecular liquid. The approach can be generalized to treat colloidal gelation and glass melting, and other soft matter slow dynamics problems.

DOI: 10.1103/PhysRevLett.115.205702 PACS numbers: 64.70.Q-, 64.70.P-, 83.10.Pp

The fundamental question of the role of attractive forces in determining the slow dynamics of crowded systems is crucial in diverse soft matter contexts [1–12]. Strong, short range attractions can trigger aggregation, gelation, and emergent elasticity in colloidal, protein, and macromolecular systems [1–4]. The role of slowly varying attractive forces in supercooled liquid dynamics and glass formation is also a critical open question [5–12]. For all these systems, the construction of a predictive microscopic theory that accurately incorporates attractive forces remains a major challenge. In this Letter we formulate a new statistical dynamical approach broadly relevant to these problems. For concreteness, and because of its fundamental interest, we focus on supercooled liquids.

Given the van der Waals (vdW) idea that the equilibrium structure of nonassociated liquids is dominated by the repulsive branch of the interparticle potential [13–15], one might expect repulsions dominate slow dynamics. However, recent constant volume simulations [6–9] of binary sphere mixtures, which probe the initial ~5 orders of magnitude of slowing down, have challenged this idea. They found that the Lenard-Jones (LJ) liquid and its Weeks-Chandler-Andersen (WCA) analog, that contains only the repulsive branch of the potential, indeed exhibit nearly identical equilibrium structure, but at lower liquid-like densities and temperatures the attractive forces slow down relaxation in a nonperturbative manner [6–9]. Key findings include the following [6–9]. (i) The large dynamical differences between the LJ and WCA liquids decrease, and ultimately vanish, as the fluid density is significantly increased. (ii) At relatively high temperatures, an apparent Arrhenius behavior is found for both systems over roughly one decade in time with a barrier that grows as a power law with density. (iii) LJ liquid relaxation times at different densities collapse by scaling temperature with the high temperature activation barrier, but such a collapse fails for the WCA fluid. (iv) The "onset" temperature at which apparent Arrhenius behavior begins to fail scales with the Arrhenius barrier height [8].

The above simulation findings have been argued [5,9] to contradict all existing force-level "microscopic" theories [e.g., mode coupling theory (MCT) [16,17], nonlinear Langevin theory (NLE) [18]], and thus pose a major open problem in glass physics. It was suggested [9] that the origin of this failure might be their neglect of higher order than pair correlations. Subsequent simulations found temperature-dependent triplet static correlations do differ for LJ and WCA fluids [19]. Moreover, the "point-to-set" equilibrium length scale (determined by beyond pair correlation function information) correlates well with the dynamical differences of the two fluids [20].

In this Letter we re-formulate the starting point for constructing microscopic dynamic theories to explicitly treat attractive forces at the simplest pair correlation level. The key new idea is to analyze the slowly relaxing component of the force-force time correlation function associated with caging directly in terms of the bare forces in real space. This avoids replacing Newtonian forces by effective potentials determined solely by pair structure, a ubiquitous approximation [15–18] that results in theories that are effectively "blind" to the dynamical differences between WCA and LJ liquids [7,9]. The predictions of our approach are in good agreement with isochoric simulations [6–9,11] and isobaric experiments on molecular liquids [21–23].

The foundation, or starting point, for many microscopic dynamical theories is the force-force time correlation function, $K(t) = \langle \vec{f}_0(0) \cdot \vec{f}_0(t) \rangle$, where $\vec{f}_0(t)$ is the total force on a tagged spherical particle due to its surroundings [16–18,24]. Its calculation involves the full many body

dynamics and thus a closure approximation must be formulated. In the ideal MCT and single particle naïve MCT (NMCT) [16,17], the standard closure projects real forces onto the slow bilinear density mode, and four point correlations are factorized into products of pair correlations in a Gaussian manner, which in Fourier space yields

$$K(t) = \frac{\beta\rho}{3}\int \frac{d\vec{k}}{(2\pi)^3}|\vec{M}(k)|^2 S(k)\Gamma_s(k,t)\Gamma_c(k,t), \quad (1)$$

where $\beta = 1/k_BT$ is the inverse thermal energy, ρ is the fluid number density, $S(k) = 1 + \rho h(k)$ is the static structure factor, $h(r) = g(r) - 1$ is the nonrandom part of the pair correlation function $g(r)$, and $\Gamma_s(\Gamma_c)$ is the single particle (collective) dynamic structure factor normalized to unity at $t = 0$. Real forces are replaced by an effective force vertex $\vec{M}(k)$ in Eq. (1) determined entirely by $g(r)$ or $S(k)$ [17]:

$$\vec{M}_{\mathrm{NMCT}}(k) = kC(k)\hat{k}, \quad (2)$$

where the direct correlation function $C(k) = \rho^{-1}[1 - S^{-1}(k)]$ and the real space effective force is $k_BT\vec{\nabla}C(r)$. Use of the projection idea implies the dramatic dynamical differences of dense WCA and LJ fluids found in the simulations cannot be captured.

To explicitly include the bare forces we reformulate the dynamical vertex of NMCT based on an alternative idea we call the projectionless dynamics theory (PDT). Inspiration comes from prior work in chemical and polymer physics in the normal liquid regime [25–27]. Technical details are in the Supplemental Material [28], but the essential idea is to first analyze the force-force time correlation function in real space as

$$K(t) = \frac{\beta}{3}\int d\vec{r}\int d\vec{r}'\,\vec{f}(r)\bullet\vec{f}(r')\langle\rho_2(\vec{r},0)\rho_2(\vec{r}',t)\rangle$$
$$= \frac{\beta}{3}\int d\vec{r}\int d\vec{r}'\,\vec{f}(r)\bullet\vec{f}(r')\rho^2 g(r)g(r')\Gamma(\vec{r},\vec{r}',t), \quad (3)$$

where $\vec{f}(r) = -\vec{\nabla}u(r)$ is the interparticle force (where r is now a field variable), $\rho_2(\vec{r},t)$ is the instantaneous fluid density a distance $\vec{r}$ from a tagged particle at the origin, at time t, and $\langle\rho_2(\vec{r},t)\rangle = \rho g(r)$. The object $\Gamma \equiv \langle\Delta\rho_2(\vec{r},0)\Delta\rho_2(\vec{r}',t)\rangle/(\langle\rho_2(r)\rangle\langle\rho_2(r')\rangle)$ is a multipoint space-time correlation of fluid collective density fluctuations *in the vicinity* of the tagged particle *relative to* the average density inhomogeneity, where $\Delta\rho_2(\vec{r},t) \equiv \rho_2(\vec{r},t) - \rho g(r)$; it is approximated by its bulk liquid form factorized to the pair correlation level [25,26]. The resulting $K(t)$ then has *exactly* the same form as Eq. (1) but with a different force vertex given by

$$\vec{M}_{\mathrm{PDT}}(k) = \int d\vec{r}g(r)\vec{f}(r)e^{-i\vec{k}\cdot\vec{r}}, \quad (4)$$

which is a Fourier-resolved structurally averaged Newtonian force. The qualitatively new feature is that the real forces now directly enter, and thus identical equilibrium pair structure does *not* imply identical dynamics.

The slow dynamics experimentally probed in the deeply supercooled regime, and also the precursor regime accessible to simulation, involves activated motion [6–9,32]. Thus, to implement the PDT idea requires a theory of activated relaxation formulated at the level of forces. We employ the well-tested "elastically collective nonlinear Langevin equation" (ECNLE) theory [33,34]. Based on using the NMCT force vertex, this approach has been shown to accurately capture alpha relaxation in hard sphere fluids and colloidal suspensions over 5–6 decades [33], and molecular liquids over 14 decades based on adopting a lightly coarse-grained mapping to an effective hard sphere fluid [34]. Relevant technical details are reviewed in the Supplemental Material [28]. Briefly, the key physical idea is that knowledge of the slowly decaying component in time of the force memory function in Eq. (1), when combined with the local equilibrium approximation that two particles move relative to each other in a manner that preserves their spatial correlation as determined by $g(r)$, allows for the self-consistent construction of the effective force a single particle experiences due to its local environment as a function of its *instantaneous* scalar displacement, r. This effective force is written as the gradient of a (defined) "dynamic free energy," $-\partial F_{\mathrm{dyn}}(r)/\partial r$, which enters a stochastic NLE for the tagged particle trajectory. Integration of this force yields $F_{\mathrm{dyn}}(r)$. Longer range collective effects enter via the cooperative elastic distortion of the surrounding fluid [35] required to accommodate the irreversible, large amplitude local hopping event described by $F_{\mathrm{dyn}}(r)$ [33,34]. The alpha relaxation event has a mixed local-nonlocal character, with a total barrier determined by coupled cage and elastic contributions computed from the dynamic free energy. The alpha time is identified as the mean barrier hopping time computed [18,33] using Kramers theory [24]. Crucially, in the PDT framework the basic structure of the ECNLE approach remains *unchanged*, but the fundamental starting point is now Eqs. (1) and (4), not Eq. (1) and Eq. (2). Thus, both pair structure and bare forces influence all aspects of the theory.

We first compare PDT theory predictions for the hard sphere fluid to its analog based on Eq. (2). We find that the NMCT and PDT force vertices for the local $kd > 2\pi$ regime are analytically *identical* for dense fluids, $M(k) \propto g(d)\cos(kd)/(kd)$ [36]. The full numerical treatment reveals that both theories predict qualitatively identical density-dependent alpha relaxation times. Quantitatively, use of the NMCT force vertex yields results that agree better with experiment and simulation [37] (see the Supplemental Material [28]).

For thermal liquids with attractive interactions, we propose a hybrid approach, in analogy with prior successful microscopic theories of diverse dynamical phenomena that treat the repulsive and slowly varying attractive forces differently [25–27]. Specifically, we adopt the NMCT vertex for repulsive forces and the PDT vertex for attractive forces

$$|\vec{M}(k)|^2 \approx k^2 C^2(k) + \left| \int d\vec{r}\, g(r)\, \vec{f}_{\rm att}(r) e^{-\vec{k}\cdot\vec{r}} \right|^2, \qquad (5)$$

where $\vec{f}_{\rm att}$ is the attractive part of the LJ force. For the WCA fluid, only the first term is present. For LJ liquids, the cross term in Eq. (5) is dropped for multiple reasons. (a) It is the simplest (seemingly inevitable) approximation consistent with the use of different dynamic closures for repulsive and attractive forces. (b) Physically, one expects cross correlations are weak since for vdW liquids the attractive and repulsive forces vary on different length scales [25]. (c) The PDT approximation for $\Gamma(\vec{r}-\vec{r}', t)$ is known to be more accurate for slowly varying attractions than harsh repulsions [25].

To implement the theory, the WCA repulsion is mapped to an effective hard sphere using the Barker-Henderson (BH) [15,38] expression $d_{\rm eff} = \int_0^{2^{1/6}} dr[1 - e^{-\beta u_{\rm WCA}(r)}]$. This mapping is reliable based on recent simulations [22]. Fluid structure is computed using Percus-Yevick (PY) theory [15] with a temperature-dependent effective packing fraction, $\eta_{\rm eff}(T) = [d_{\rm eff}(\beta\varepsilon)/\sigma]^3\eta$, where $\eta \equiv \pi\rho\sigma^3/6$, and ε and σ are the LJ energy and length scale, respectively. To isolate the dynamical consequences of attractive forces, the literal vdW picture that $g(r)$ of the LJ and WCA liquids are identical is adopted [13–15]. While the BH mapping and PY theory become less accurate at high densities, no qualitative changes to our results are expected if alternative approximations are employed. Moreover, neither accurate integral equation theory nor simulation data for the WCA $g(r)$ of a *one*-component liquid in the (deeply) supercooled regime are available. Most importantly, the essential leading order origin of our new results is *not* related to pair structure, but rather the explicit accounting for attractive forces on slow dynamics.

Under isochoric conditions, ρ and η are fixed, but $\eta_{\rm eff}$ grows with cooling via $d_{\rm eff}(\beta\varepsilon)$. Representative calculations are shown in Fig. 1 for $\eta = 0.48$ and $\eta = 0.54$. For $\eta = 0.48$, the LJ fluid relaxes much slower than its WCA fluid analog at lower temperatures. As η increases, these differences smoothly decrease (not shown), and the relaxation times of the two systems are nearly identical at $\eta = 0.54$. These results are in accord with the simulation trends [6–9]. To develop an intuitive understanding, we compute the long wavelength [$k = 0$ in Eq. (4)] effective forces that enter the vertex: $M_{\infty,R} \equiv 4\pi k_B T d_{\rm eff}^2 g(d_{\rm eff})$ for repulsions and $M_{\infty,A} = \int d\vec{r} g(r) f_{\rm att}(r)$ for attractions. The inset of Fig. 1 shows that for $\eta = 0.48$ the repulsive forces dominate at high temperatures where the LJ and WCA relaxation times are similar. The attractive force contribution grows faster than the repulsive analog with cooling and ultimately dominates, consistent with the main frame results. For $\eta = 0.54$ the repulsions dominate at all temperatures.

As seen in simulation [6–9], Fig. 1 shows that an apparent Arrhenius behavior is predicted at high temperature which is physically due to the unimportance of the collective elasticity aspect of the alpha relaxation process

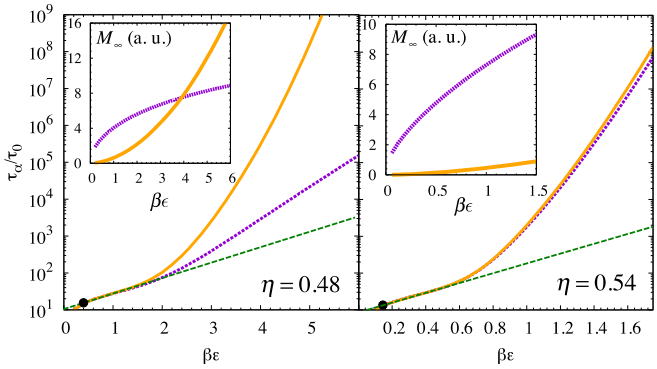

FIG. 1 (color online). Nondimensionalized alpha relaxation times for the LJ (orange, solid) and WCA (purple, dashed) fluids at two packing fractions as a function of dimensionless inverse temperature. For thermal systems, $\tau_0 \equiv (24\rho\sigma^2)^{-1}\sqrt{M/\pi k_B T}$, where M is the particle mass [33]. The black points denote the predicted emergence of a barrier (ideal NMCT crossover), while the green dashed line shows the high temperature Arrhenius behavior. (Inset) The average effective attractive (orange, solid) and repulsive (purple, top curve at small $\beta\epsilon$) contributions to the force vertex, in arbitrary units, for the same packing fractions.

[34]. One can ask whether the theoretical relaxation times for different packing fractions collapse if temperature is scaled by the apparent Arrhenius barrier, $E_\infty(\eta)$. In agreement with simulations [6,8], for WCA fluids no collapse is found (see the Supplemental Material [28]), but for LJ fluids Fig. 2 shows an excellent collapse over 7 decades. The inset shows the Arrhenius barriers are nearly identical for both fluids, and grow as $\beta E_\infty \propto \eta^{9.3}$. The high apparent power law exponent (simulation [6] finds ~5) is expected if the continuous repulsion is replaced by an effective hard sphere potential [10]; our exponent value is in excellent agreement with simulations that explored consequences of

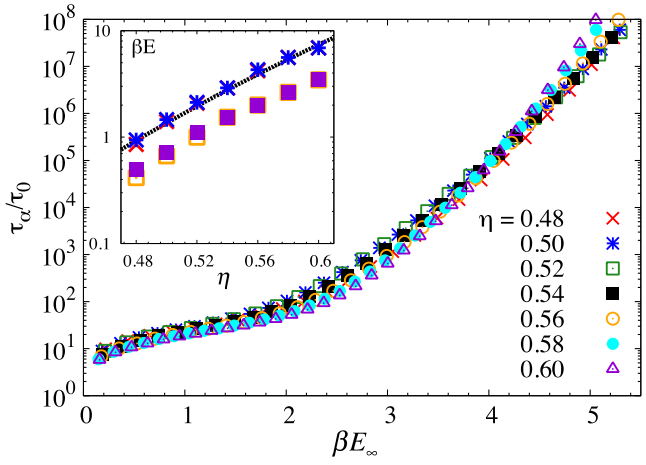

FIG. 2 (color online). Collapse of the nondimensionalized alpha times for the isochoric LJ systems at different packing fractions. Temperature is scaled by the apparent Arrhenius barrier, $E_\infty(\eta)$. (Inset) βE_∞ for LJ (blue, stars) and WCA (red, crosses) fluids (almost indistinguishable), compared to the onset temperature $k_B T_{\rm onset}$ (LJ, purple, closed squares; WCA, orange, open squares). The black dashed line is the power law $\beta E_\infty \propto \eta^{9.3}$.

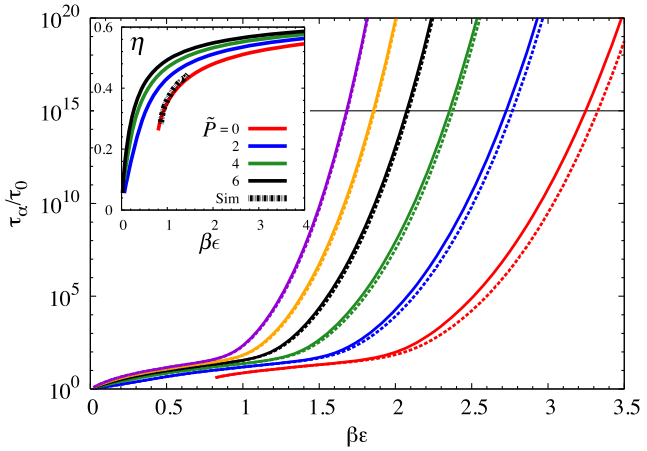

FIG. 3 (color online). Dimensionless mean alpha times for LJ (solid) and WCA (dashed) fluids as a function of scaled inverse temperature at reduced pressures (right to left) of $\tilde{P} = 0$, 2, 4, 6, 8, 10. The horizontal line illustrates the kinetic vitrification based on $\tau_\alpha(T_g) = 100$ s and $\tau_0 = 0.1$ ps. (Inset) Model equation of state results (curves; see the Supplemental Material [28]) for $\tilde{P} = 0$, 2, 4, 6 (right to left). The black hashed curve shows the fit to simulation data [39] of the one-component LJ fluid and should be compared to the $\tilde{P} = 0$ (red) curve.

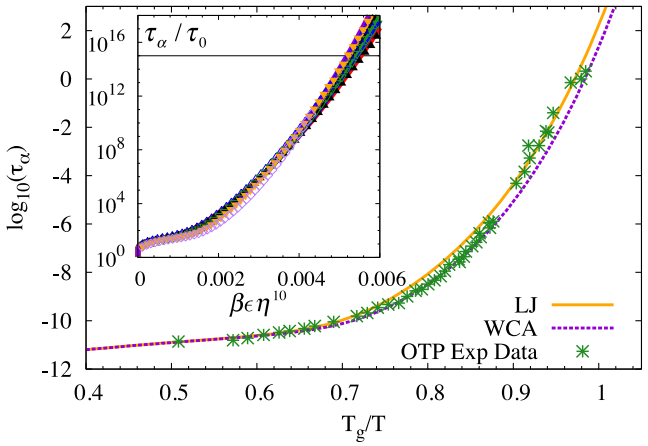

FIG. 4 (color online). Logarithm of the mean alpha time (in seconds) vs reduced inverse temperature for the LJ (orange, solid) and WCA (purple, dashed) fluids at $\tilde{P} = 0$, compared to experimental OTP data (green stars) [23]. The theory curves are shifted vertically to match the high temperature experimental relaxation times. (Inset) Collapse of the dimensionless alpha times for $\tilde{P} = 0$, 2, 4, 6, 8, 10 (curves) and isochoric $\eta = 0.50, 0.52, 0.54, 0.56, 0.58$ (points) conditions with the reduced variable $\beta\epsilon\eta^{10}$. The horizontal line has the same meaning as in Fig. 3.

the WCA to hard sphere mapping [22]. We have also computed an "onset temperature," $T_{\rm on}$, defined as when the apparent Arrhenius behavior first fails. From Fig. 2 we find $E_\infty \approx 2k_BT_{\rm on}$, consistent with simulation [6–9]. All the theoretical results discussed above are in good agreement with the trends found in the isochoric simulations performed in the dynamic precursor regime [6–9].

Isochoric simulations have also shown that a system interacting via a repulsive inverse power law (IPL) potential, $u_{\rm IPL}(r) = A\epsilon(\sigma/r)^n$, has the same $g(r)$ as the LJ fluid if A and ϵ are properly tuned [11]. The relaxation times of the LJ and IPL fluids are then found to be nearly identical [11]. In the Supplemental Material [28] we show that our theory is consistent with this "hidden scale invariance" feature and the idea that the dynamical differences between the LJ and WCA fluids is repulsive force truncation [10,11].

We now consider experimental systems, which are typically studied at constant pressure and over 14 or more decades in relaxation time [21,23,32]. We employ a model LJ equation of state [39] (see the Supplemental Material [28]) to perform constant reduced pressure ($\tilde{P} \equiv \beta P\sigma^3$) calculations. The effective packing fraction of the reference hard sphere fluid now varies with temperature due to both an increase of effective particle size $d_{\rm eff}$ with cooling and thermal contraction (η increases). Results for the *dynamically* LJ and WCA fluids (with the *same* structural input) are shown in Fig. 3. The two fluids have nearly identical relaxation times. At atmospheric pressure ($\tilde{P} = 0$), a one-decade difference is visible, which vanishes as pressure increases because density grows with cooling (Fig. 3, inset).

Quantitative contact with isobaric experiments is made based on Fig. 3. A kinetic vitrification temperature T_g is defined as when $\tau_\alpha(T_g) \equiv 10^{15}\tau_0 \simeq 100s$ for a typical $\tau_0 \simeq 0.1$ ps (horizontal line in Fig. 3). For LJ liquids at atmospheric pressure we find $k_BT_g = 0.31\epsilon$, and a fragility of $m_{P=1\rm atm} = 62$ significantly larger than its isochoric analog of $m_V \approx 26$. This fragility difference is consistent with experiment [21]. For the LJ liquid, the theory also properly predicts T_g increases and fragility decreases with pressure (not shown). The vdW liquid orthoterphenyl (OTP) has roughly $\epsilon/k_B \approx 700$ K [40,41]. Using this, we obtain $T_g = 216$ K, in reasonable accord with the experimental $T_g = 246$ K [21,23]. Figure 4 demonstrates that the full relaxation time profiles in the reduced inverse temperature Angell representation (vertically shifted to match the high temperature OTP Arrhenius data [23]) are in excellent agreement with experiment.

The inset of Fig. 4 attempts to collapse *both* the isobaric and isochoric LJ liquid relaxation times over a wide range of densities and pressures. The result is consistent with density-temperature scaling [10,21]. The inset also shows that the density scaling exponent is high (~10), consistent with recent simulations that mapped WCA repulsions to effective hard spheres [22] and as expected based on isomorph theory [10–12].

In conclusion, a new approach for constructing microscopic force-based theories of slow dynamics that explicitly includes attractive forces has been developed at the level of pair correlations. Under isochoric conditions, the attractive forces can have a major effect on supercooled liquid dynamics but as density increases their influence vanishes, as previously concluded based on a very different analysis [42]. Under isobaric conditions, attractive forces are much less important due to thermal contraction. Our results are consistent with recent simulations [6–9] and experiments [21,23]. The

theoretical approach can be applied to more complex soft matter systems. For example, colloidal gels where strong and short range attractive forces induce transient bonding [3], which is explicitly described at the force level using PDT. Although beyond the scope of this Letter, we do find that the essential features of the "re-entrant glass melting" phenomenon induced by a short range attraction [3,43] is captured by the PDT-ECNLE approach, as briefly discussed in the Supplemental Material [28]. More generally, the new force vertex idea can be employed in the dynamic free energy framework previously applied to study activated dynamics in glass and gel forming materials composed of nonspherical colloids [44,45], polymers [46], and soft repulsive colloids [47].

This work was supported by DOE-BES under Grant No. DE-FG02-07ER46471 administered through the Frederick Seitz Materials Research Laboratory. Helpful discussions with Ryan Jadrich and Anh Phan are gratefully acknowledged. We thank John McCoy for bringing Ref. [22] to our attention.

*kschweiz@illinois.edu

[1] D. Leckband and J. Israelachvili, Q. Rev. Biophys. **34**, 105 (2001).
[2] D. Kushner, Microbiol. Mol. Biol. Rev. **33**, 302 (1969).
[3] E. Zaccarelli, J. Phys. Condens. Matter **19**, 323101 (2007).
[4] J. Bergenholtz and M. Fuchs, Phys. Rev. E **59**, 5706 (1999).
[5] J. P. Bouchaud, Commentary for Journal Club for Condensed Matter Physics, http://www.condmatjournalclub.org/?p=1022 (June 22, 2010).
[6] L. Berthier and G. Tarjus, Phys. Rev. Lett. **103**, 170601 (2009).
[7] L. Berthier and G. Tarjus, Phys. Rev. E **82**, 031502 (2010).
[8] L. Berthier and G. Tarjus, J. Chem. Phys. **134**, 214503 (2011).
[9] L. Berthier and G. Tarjus, Eur. Phys. J. E **34**, 96 (2011).
[10] J. C. Dyre, J. Phys. Chem. B **118**, 10007 (2014).
[11] U. R. Pedersen, T. B. Schrøder, and J. C. Dyre, Phys. Rev. Lett. **105**, 157801 (2010).
[12] L. Bøhling, A. A. Veldhorst, T. S. Ingebrigtsen, N. P. Bailey, J. S. Hansen, S. Toxvaerd, T. B. Schrøder, and J. C. Dyre, J. Phys. Condens. Matter **25**, 032101 (2013).
[13] J. D. Weeks, D. Chandler, and H. C. Andersen, J. Chem. Phys. **54**, 5237 (1971).
[14] B. Widom, Science **157**, 375 (1967).
[15] J. P. Hansen and I. R. McDonald, *Theory of Simple Liquids* (Academic, London, 1986).
[16] W. Götze, *Complex Dynamics of Glass-Forming Liquids: A Mode-Coupling Theory* (Oxford University Press, New York, 2008).
[17] T. R. Kirkpatrick and P. G. Wolynes, Phys. Rev. A **35**, 3072 (1987).
[18] K. S. Schweizer, J. Chem. Phys. **123**, 244501 (2005).
[19] D. Coslovich, J. Chem. Phys. **138**, 12A539 (2013).
[20] G. M. Hocky, T. E. Markland, and D. R. Reichman, Phys. Rev. Lett. **108**, 225506 (2012).
[21] R. Casalini, K. J. McGrath, and C. M. Roland, J. Non-Cryst. Solids **352**, 4905 (2006); C. Roland, S. Hensel-Bielowka, M. Paluch, and R. Casalini, Rep. Prog. Phys. **68**, 1405 (2005).
[22] J. Budzien, J. V. Heffernan, and J. D. McCoy, J. Chem. Phys. **139**, 244501 (2013).
[23] E. Rössler, U. Warschewske, P. Eiermann, A. Sokolov, and D. Quitmann, J. Non-Cryst. Solids **172**, 113 (1994).
[24] R. Zwanzig, *Nonequilibrium Statistical Mechanics* (Oxford University Press, New York, 2001).
[25] K. S. Schweizer and D. Chandler, J. Chem. Phys. **76**, 2296 (1982).
[26] K. S. Schweizer, J. Chem. Phys. **91**, 5802 (1989).
[27] S. A. Rice and P. Gray, *The Statistical Mechanics of Simple Liquids* (Wiley Interscience, New York, 1965).
[28] See Supplemental Material at http://link.aps.org/supplemental/10.1103/PhysRevLett.115.205702 for details of the model equation-of-state employed, the PDT and ECNLE theories, and additional calculations for the hard sphere, WCA, inverse power law, and sticky colloidal systems, which includes Refs. [29–31].
[29] E. J. Saltzman and K. S. Schweizer, J. Chem. Phys. **125**, 044509 (2006).
[30] E. Zaccarelli, J. Phys. Condens. Matter **19**, 323101 (2007); A. M. Puertas, M. Fuchs, and M. E. Cates, Phys. Rev. Lett. **88**, 098301 (2002); F. Sciortino, Nat. Mater. **1**, 145 (2002).
[31] Z. E. Dell, A. Phan, and K. S. Schweizer (unpublished).
[32] A. Cavagna, Phys. Rep. **476**, 51 (2009); L. Berthier and G. Biroli, Rev. Mod. Phys. **83**, 587 (2011).
[33] S. Mirigian and K. S. Schweizer, J. Chem. Phys. **140**, 194506 (2014).
[34] S. Mirigian and K. S. Schweizer, J. Phys. Chem. Lett. **4**, 3648 (2013); J. Chem. Phys. **140**, 194507 (2014).
[35] J. C. Dyre, J. Non-Cryst. Solids **235**, 142 (1998); Rev. Mod. Phys. **78**, 953 (2006).
[36] K. S. Schweizer and G. Yatsenko, J. Chem. Phys. **127**, 164505 (2007).
[37] G. Brambilla, D. El Masri, M. Pierno, L. Berthier, L. Cipelletti, G. Petekidis, and A. B. Schofield, Phys. Rev. Lett. **102**, 085703 (2009).
[38] J. A. Barker and D. Henderson, J. Chem. Phys. **47**, 4714 (1967).
[39] G. S. Boltachev and V. G. Baidakov, High Temp. **41**, 270 (2003).
[40] ϵ_{OTP} is roughly estimated from the known value for benzene ($\epsilon_{\mathrm{benz}}/k_B = 377$ K) by using the vdW idea that it is proportional to the boiling temperature $T_{\mathrm{boil}} \propto \epsilon$, and the ratio $T_{B,\mathrm{OTP}}/T_{B,\mathrm{benz}} \approx 2$.
[41] F. Cuadros, I. Cachadina, and W. Ahumada, Molecular engineering **6**, 319 (1996).
[42] Y. S.Elmated, D. Chandler, and J. P.Garrahan, J. Phys. Chem. B **114**, 17113 (2010).
[43] K. N. Phan *et al.*t, Science **296**, 104 (2002); D. R. Reichman, E. Rabani, and P. L. Geissler, J. Phys. Chem. B **109**, 14654 (2005); L. J. Kaufman and D. A. Weitz, J. Chem. Phys. **125**, 074716 (2006).
[44] M. Tripathy and K. S. Schweizer, Phys. Rev. E **83**, 041406 (2011); J. Chem. Phys. **130**, 244906 (2009).
[45] R. Zhang and K. S. Schweizer, Phys. Rev. E **80**, 011502 (2009); **83**, 060502R (2011).
[46] S. Mirigian and K. S. Schweizer, Macromolecules **48**, 1901 (2015).
[47] J. Yang and K. S. Schweizer, Europhys. Lett. **90**, 66001 (2010); J. Chem. Phys. **134**, 204908 (2011).